
Synthetic Aperture Radar Observations of Ocean and Land

R. K. Raney

Phil. Trans. R. Soc. Lond. A 1983 **309**, 315-321

doi: 10.1098/rsta.1983.0044

Email alerting service

Receive free email alerts when new articles cite this article - sign up in the box at the top right-hand corner of the article or click [here](#)

To subscribe to *Phil. Trans. R. Soc. Lond. A* go to: <http://rsta.royalsocietypublishing.org/subscriptions>

Synthetic aperture radar observations of ocean and land

BY R. K. RANEY

*Canada Centre for Remote Sensing, Department of Energy, Mines and Resources,
2464 Sheffield Road, Ottawa, Canada K1A 0Y7*

[Plates 1–4]

A brief history of synthetic aperture radar (SAR) from early radar ideas to recent satellite systems is presented. Properties of electromagnetic radar measurement that are fundamental to SAR systems are presented and discussed by the use of example SAR images derived from airborne and Seasat satellite sources. The next decade of activity in radar satellites is outlined.

1. BACKGROUND

The first patent for a rudimentary radar was issued to Hulsmeyer (Germany) in 1904. There were several technically successful but financially weak developments of special related devices over the next 30 years, but it required the threat of World War II to motivate real progress. Robert Watson-Watt proposed to the British Government in 1934 the principle of aircraft detection by ground-based pulsed radar, and described in detail how it could be done. By the spring of 1935 an experimental system proved to be successful, leading to the construction of the British Home Chain, which saw five stations operational in 1938, a major technological accomplishment.

The development of radar during World War II was explosively rapid, aided by high-level technical exchange agreements amongst the Allies. The range and sensitivity of radars were constantly improved, and smaller units were built for shipborne and airborne use.

These developments required higher power and shorter wavelengths than previously available. Whereas the work in 1935 was at $\lambda = 25$ m, sensitivity, size and performance requirements led to wavelengths as short as $\lambda = 10$ cm by 1940, thus initiating microwave radar. The pulsed high-power transmission requirement was met by the development of the cavity magnetron by John T. Randal & Henry A. Boot (University of Birmingham) during 1939–41, achieving peak pulse powers on the order of 500 kW.

The development of radar by the Allies was very tightly classified during World War II. For that reason, the several wavelengths in use received code names, in use to this day. Thus we have inherited the following: L-band (25 cm), S-band, (10 cm), C-band (5 cm), X-band (3 cm), and K-band (1 cm) in the popular microwave portion of the spectrum. Shorter waves are used by 'millimetre radars'.

The close of World War II found aircraft equipped with radars that displayed on a 'plan position indicator' (PPI) a 360° image of the terrain below the aircraft. Towards 1950 a modification of this approach led to a side-looking radar known as SLAR (side-looking airborne radar). The radar antenna in this case, rather than spinning around through 360°, was kept pointing to one side and the resulting imagery was that of the terrain parallel to the aircraft. The quality

[73]

of this imagery could be improved in resolution by shortening the range pulse, but the cross range or azimuth resolution was difficult to improve. Angular resolution is limited by the well known Rayleigh or diffraction limit, for which better performance requires a larger aperture. It is at this point that the logical development of synthetic aperture radar (SAR) begins.

An antenna carried on an aircraft or satellite cannot be made very large, thus apparently limiting the azimuth resolution. However, if the received energy could be recorded in memory for a set of successive scan lines, then perhaps the data in memory could be processed to achieve a much improved azimuth resolution, just as if those same scan lines had been simultaneously collected by a much larger antenna. This observation, first proposed by Carl Wiley of Goodyear Aerospace Corporation in 1954, lies at the heart of the synthetic aperture approach. The resulting theoretical azimuth resolution is $\rho = \frac{1}{2}d$ for an antenna of aperture size d .

Note that the diffraction-limited azimuth resolution of the synthetic aperture is not a function of wavelength and is improved as the aperture d is made smaller. Both of these facts are in distinct contrast to the conventional diffraction-limited approach to a real aperture system. Note also that SAR azimuth resolution is not a function of range, and thus this radar technique is an ideal candidate for satellite applications.

There are four conditions that must be met by a side-looking radar sensor system for the resulting signal to yield successfully to synthetic resolution (see figure 1).

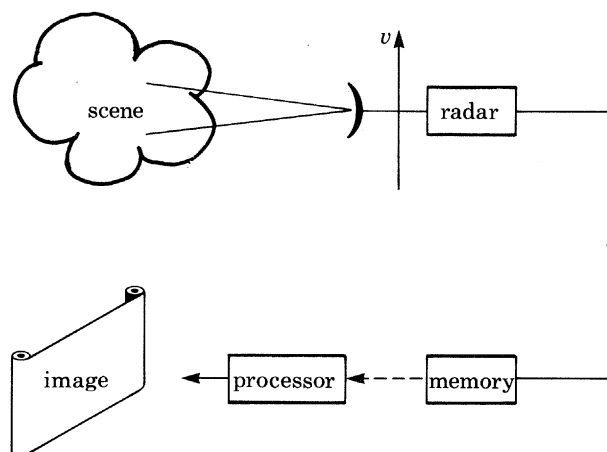


FIGURE 1. Conceptual diagram of a synthetic aperture radar.

1. Memory: the signal received at one point in time is of use in processing only in the context of all other signals received over the required synthetic aperture length. This requires a high-speed memory and in many applications a very large one at that. The memory accumulates data sequentially gathered by the radar as it traverses along the synthetic array length past the scene.

2. Processor: the set of signals must be processed to form an image. One differentiates between the signal history (input to processor) and the image itself (output from processor). For a SAR, the image processor is of importance equal to that of the radar itself, and is the most time-consuming task.

3. System coherence: individual frequencies may be processed only to the extent that they are present in memory. This requires that the wave front sampled by the radar as it traverses along the line of flight over the synthetic aperture length must have a consistent phase structure. If

there are across-track motion errors or timing errors in the system, they must be measured and compensated for, to maintain signal coherence. This usually imposes technological restraints on the radar itself, setting SAR systems apart from conventional side-looking real aperture radars.

4. Scene coherence: having a perfectly coherent radar is of no consequence if the scene or objects in it have their own random or deterministic motion. The scene itself must respect phase stability during the time over which the synthetic aperture is formed. If this condition is not satisfied then curious or disappointing results occur.

The first demonstration of an airborne SAR system was performed by the Willow Run Laboratories (now E.R.I.M.) of the University of Michigan in the late 1950s. The problem of maintaining coherence was met by the use of an inertial navigation and analogue phase-correction system. The memory and processor requirements were jointly achieved through recording the signals onto photographic film, which later was processed in an optical correlator.

A major improvement in the system, and a fundamental insight into its operation, was achieved by Emmett Leith. He applied the concept of an offset reference frequency (in common use in communication theory) to the wavefront reconstruction work of Dennis Gabor (first proposed by him in 1947) to arrive at the holographic view of the azimuth behaviour of a SAR. In this way, optical processing of SAR data was both simplified and established as the standard technique, essentially unchallenged until 1978. During that time, several experimental SAR systems were built at X, L, and S-bands; the military adopted X-band and developed production SAR for a variety of roles.

In 1978 the U.S.A. launched the first (and so far the only) satellite to carry a SAR system. Seasat as a proof-of-concept mission operated from July to October 1978, at which time there was a prime power system failure. The SAR was at L-band, with a resolution of $25\text{ m} \times 25\text{ m}$ at four looks over a swath of 100 km, as seen by a nominal incidence angle of 20° from vertical.

Optical processing was the N.A.S.A. baseline plan for Seasat. However, there were independent developments of digital processing capability suitable for Seasat both in the U.S.A. and in Canada. The first digitally processed image from Seasat SAR was completed by MacDonald, Dettwiler and Associates (under funding from the Canada Sursat Project), and published in November 1978. Digital SAR processing proved to be outstanding in quality. The major remaining obstacle is speed. In 1978 it took 40 h to process one quarter frame of data, gathered by the satellite in a few seconds! The best rates currently are on the order of 2 h for one full frame of $100\text{ km} \times 100\text{ km}$.

2. IMAGE PROPERTIES

The image resulting from the processed data record collected by a SAR can be described in fundamental terms similar to more conventional passive imaging systems. The image brightness pattern is the result of a convolution of the system function (its response to an isolated point reflector) over the scene reflectivity function. Features of the image such as resolution, geometric properties, and background noise level are determined primarily by the SAR itself. Foundations for this description were set by P. M. Woodward.

Physical parameters of the surface that directly affect the image are surface roughness, dielectric constant and scene motion. Geometric parameters relating the radar and observed surface are polarization, radar wavelength and viewing angle.

Surface roughness is the most important scene characteristic determining relative reflectivity brightness, with rough surfaces appearing brighter in a side-looking radar image than smoother

surfaces. The measure of roughness is wavelength λ and incidence angle θ dependent according to the Rayleigh criterion, according to which the critical mean height variation $h_0 = \frac{1}{2}\lambda \cos \theta$, so that surfaces with variations less than h_0 appear 'smooth', and surfaces with height variations larger than h_0 appear 'rough'. As a general rule, one sees in images this effect at work, so that smooth water appears dark, most agricultural features show various shades of grey, whereas forests or major geological features are brightly represented.

Figure 2, plate 1, an image from the Seasat SAR processed digitally by M.D.A. (Canada), illustrates the differential brightness response to surface roughness. Radar data have a very wide range of intensity, even for natural surfaces, which for a scene such as this is typically two orders of magnitude.

The *complex dielectric constant* describes the electromagnetic properties of a material in quantitative terms. To first order, good conductors are good reflectors, and good insulators are poor reflectors. Most natural surfaces such as ice or vegetation are partly conducting. For these materials, microwave radiation penetrates the volume, is attenuated, and is reflected from within the material. These properties allow the possibility of measurement by SAR of certain material properties such as soil moisture, although the variable of interest is easily masked by system or roughness variations. Since for many interesting surfaces (e.g. ice) the dielectric constant is in fact a function of temperature and salt content, it is a source of unknown reflectivity variation as well as latent information. These are areas of active research in microwave remote sensing.

Figure 3, plate 2, shows the impact of rain on the reflectivity of a nominally dry region of Wyoming, as seen by Seasat in August 1978. The rain (brighter streaks) caused the dielectric constant of the surface to increase and hence the increased reflectivity.

Scene motion has impacts on imagery that are unique to SAR systems, a consequence of the time required to form the synthetic aperture along the flight track. Two classes of motion are of interest, deterministic and random.

For a discrete object with a (slowly varying) velocity, its image will be out of focus in azimuth in response to its along-track velocity component and any accelerations, and will be shifted in azimuth from its true position in proportion to its velocity towards the radar track. Figure 4, plate 3, shows the azimuthal shift of a ship's image relative to the wake of the ship. The amount of shift can be measured and reduced through the known radar viewing geometry to estimate the ship's speed accurately. The lack of such shift for waves accompanying the ship's progress is illustrative of the more subtle mechanisms that govern the formation of their images.

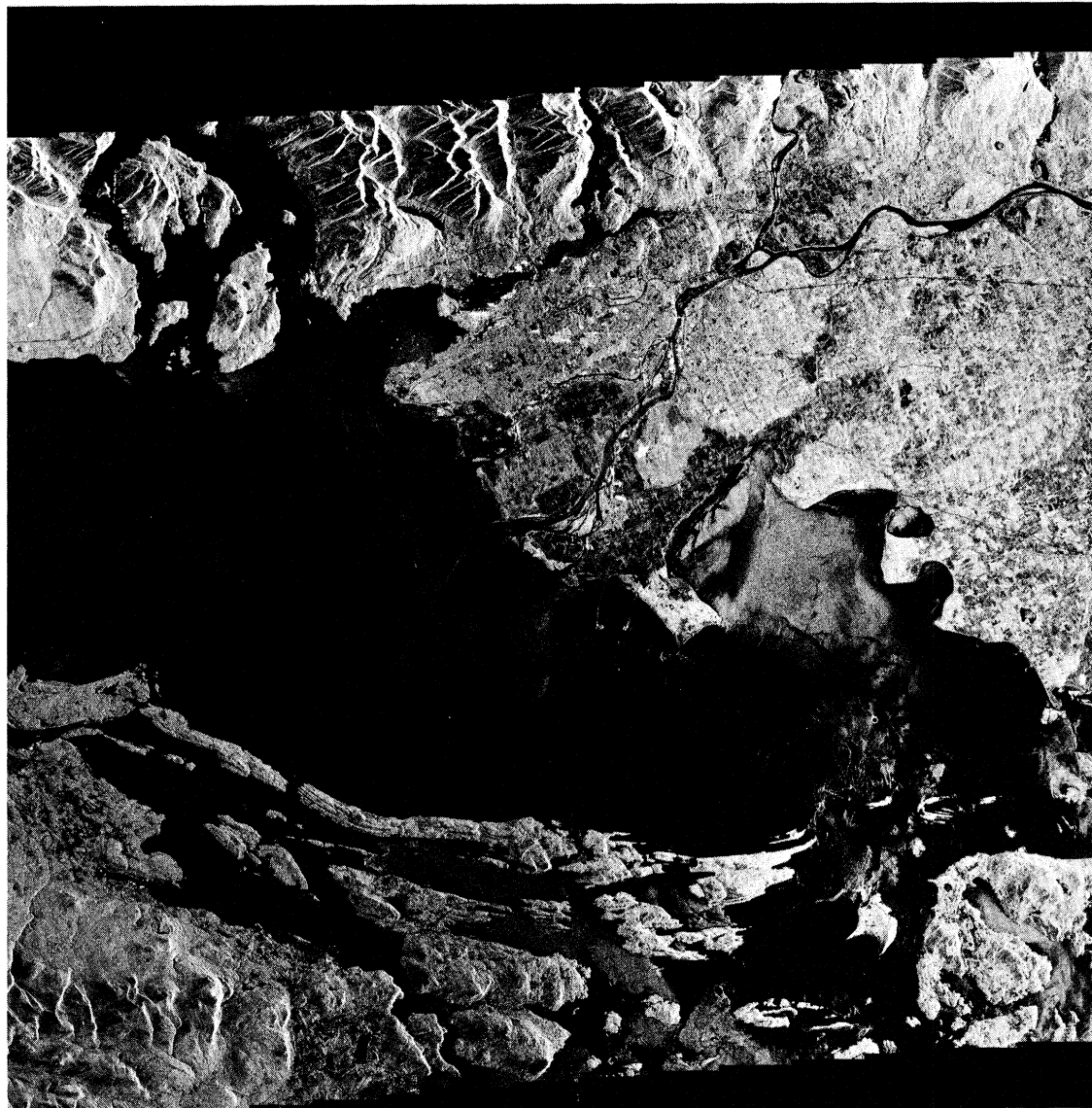
In Earth observation, random motions are of frequent occurrence, either on the surface of water bodies or wind-blown vegetation. It can be shown that the average reflectivity of such scenes is transferred to the image of a SAR unspoilt by the random motion, but that the ability of the SAR to maintain resolution is adversely affected if the scene complex correlation time is shorter than the time required by the SAR to form the aperture. This is a characteristic that frequently restricts the imaging response of a SAR to oceanic wave patterns.

One problem of oceanic wave imaging is illustrated in figure 5, plate 3, in which a swell system is propagating into a field of floating ice off the coast of Labrador. The waves are visible on the ice, but not on the water. This is due primarily to the fact that the relative time-varying complexity of the water surface reduces the ability of the SAR to achieve spatial resolution, in contrast to the conditions for the same dominant wave system in ice. This is an area of active research. (Data are from the Canadian X-band airborne SAR, and were processed optically.)

SEASAT SAR

SCALE 1:500000
FRAME CENTRE 49° 6' 42" N 123° 14' 11" W

VANCOUVER, CANADA 100X100 KM
ORBIT 230 13/07/78
25M RESOLUTION 4 LOOKS
SATELLITE HEADING 289.77 DEG
GROUND RANGE



21541
25.063

CANADA SURSAT PROJECT

DIGITALLY PROCESSED BY
DEFENCE RESEARCH ESTABLISHMENT TORONTO, CANADA

FIGURE 2. A Seasat SAR image of Vancouver, B.C.

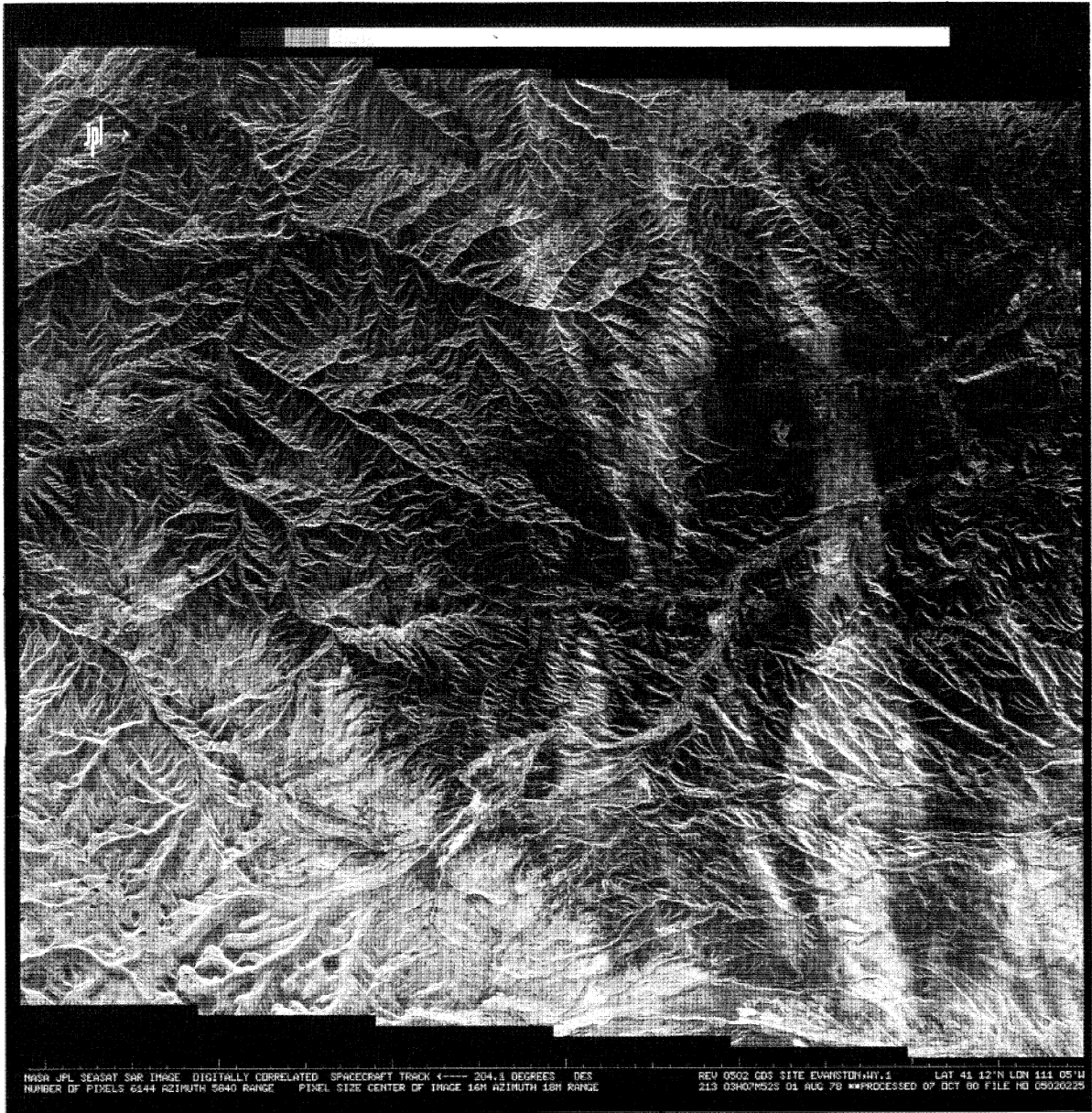


FIGURE 3. Effect of recent rain on dry terrain in Wyoming: the streaks are as a result of rain (verified by A. Loomis). Pixel size $16\text{ m} \times 18\text{ m}$. (Courtesy of N.A.S.A.)

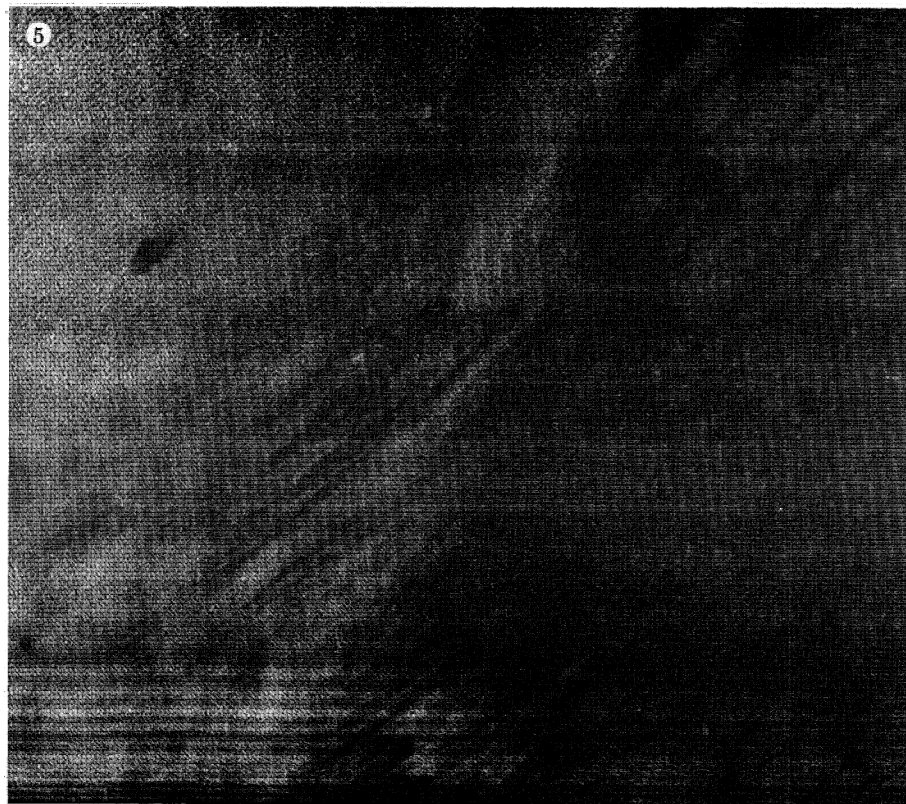
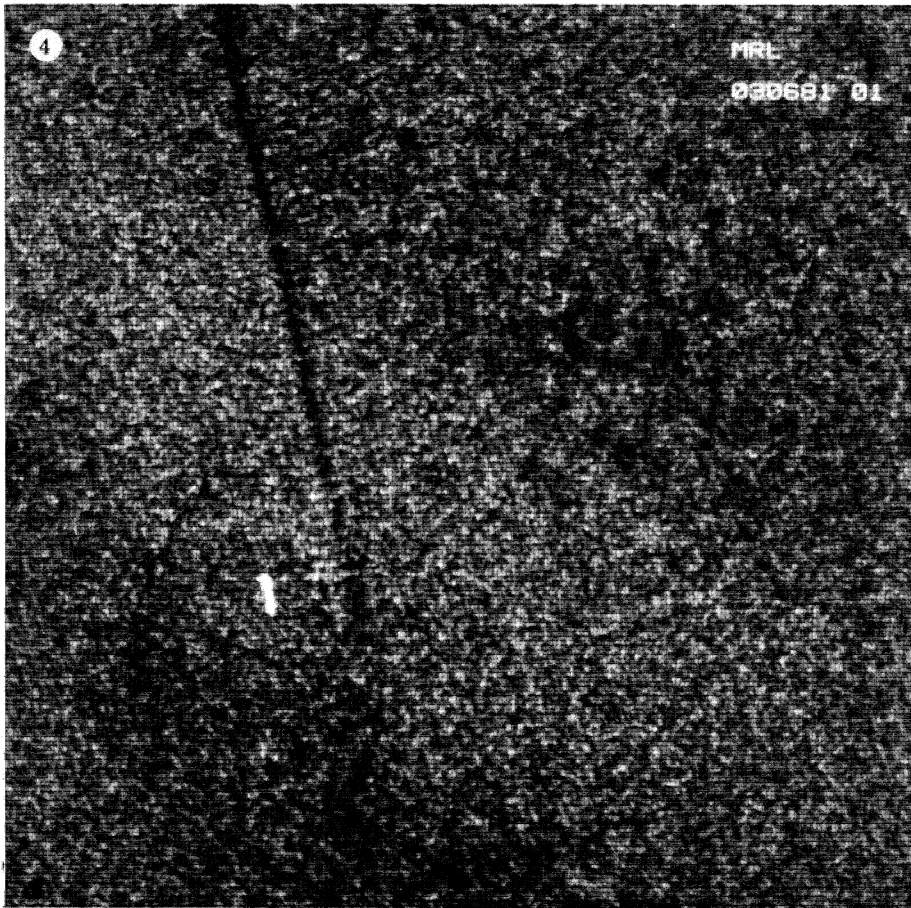


FIGURE 4. Image displacement of a ship caused by its motion (enlarged image, courtesy of Marconi Ltd).

FIGURE 5. Waves in an ice and water environment: waves are visible in the floating ice only (bottom of figure is radar near range).

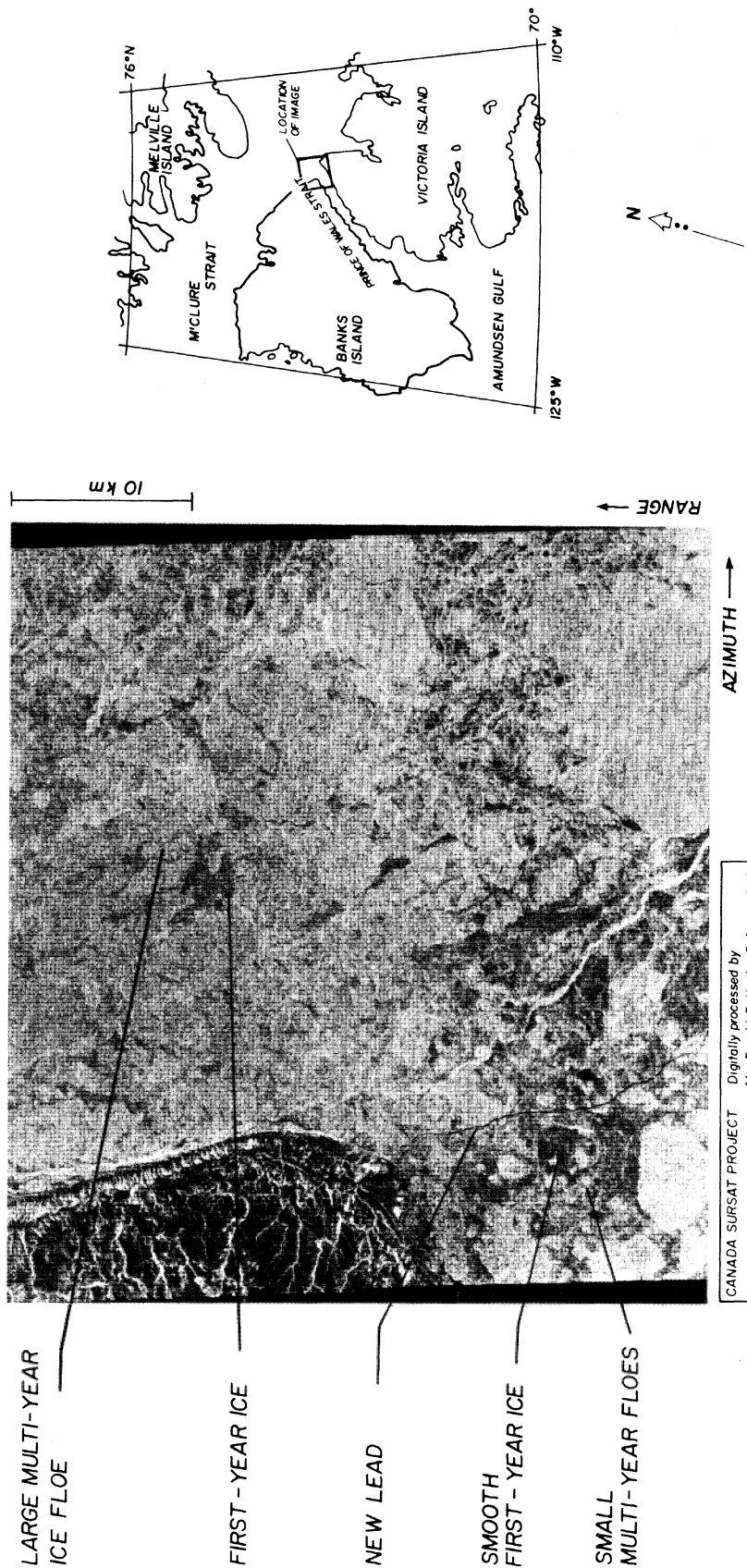


FIGURE 7. Seasat SAR image of Peel Point, N.W.T. (25 m resolution, 4 looks).

3. THE DECADE AHEAD

Worldwide, there are three free-flying Earth observation satellites planned for the next 10 years that are to carry SAR systems: ERS-1 (European Remote Sensing Satellite), Radarsat (Canada) and J-ERS-1 (Japanese Environmental Remote Sensing Satellite). The capabilities of these are in outlined table 1. The prime contractor for the ERS-1 radar system (whose acronym is AMI) is Marconi Ltd.

TABLE 1. COMPARISON OF FUTURE SATELLITE SARs

	Radarsat	ERS-1	J-ERS-1
launch	1990	1988	1988
radar band	C	C	L
processing	Par	Easier	Harder
resolution/m (looks)	25 (3)	30 (4)	25 (4)
swath width/km	ca. 150	80	75
accessible swath/km	500	80	75
incidence angle/deg	20-45	22	33
sensitivity/dB	-25	-18	?
coverage	< 76° N	< 88° N	< 80° N?
coverage interval			
at 73° N	< 1 day	> 4 days	?
downlink	digital compatible	digital compatible	digital compatible
on-board recorder	yes	no	yes

In addition, there are three shuttle imaging-radar missions planned, MRSE (Microwave Remote Sensing Experiment, the German contribution to Space lab), SIR-B (1984, N.A.S.A. approved, duration 1 week, maximum northern coverage 48° N), and an experimental SAR (1986, not approved by N.A.S.A., duration one week). This discussion does not consider these shuttle-based radars, since for operational requirements these systems are of little interest. (Although Radarsat, ERS-1 and J-ERS-1 are planned to be launched in the 1988-1990 time frame, none of these programmes are fully approved at the final build to completion commitment level.)

The advance of ERS-1 over Radarsat by 2 years is an advantage to both programmes. For Canada, a limited amount of data will be available to serve as test, validation and qualification input for ground stations, signal processors and product dissemination facilities. There will be an opportunity for user feedback and pre-operational experience. For E.S.A., there will be a genuine user 'on-line', ready to take advantage of the satellite information, thus serving as a pilot project for the validation of the satellite SAR system.

The radar system frequency has been selected to be C-band (5.3 GHz) for both the Canadian and E.S.A. systems. The Japanese system, essentially a copy of the Seasat SAR, is at L-band. The higher frequency of C-band is preferred for ice applications, based on Seasat and airborne experiments.

From an operational point of view, the two main issues are coverage and the availability of data to the user. The potential data-flow bottleneck is SAR data processing. Once processing speed is planned that is adequate to support Radarsat and Canadian users, then Canadian processing of ERS-1 data is a simple task. On the other hand, some compromises would be required to accommodate J-ERS-1 data, because L-band is more difficult to process accurately and rapidly.

The nominal swath of Radarsat is much wider than that of ERS-1 (150 km as against 80 km).

Furthermore, the Radarsat swath actually imaged can be selected (during a pass or mission if need be) anywhere within an accessibility zone 500 km wide. This has two major advantages.

1. It is possible to image any given location north of 51° N at least once every 72 h. This is of critical importance for site-specific or route-specific applications, such as shipping. This frequency of coverage, if met by a fixed swath system such as Seasat or ERS-1, would require a network of at least three satellites.

2. It is possible to gather data on subsequent orbits from one Earth location at different incidence angles, such as near 22° and near 43° . This provides a basis for an all-weather stereoscopic data set worldwide, which would be of great potential value in economic geology.

Thus it is that south of 75° N, Radarsat has substantial coverage advantages over ERS-1. This is achieved by use of swath steering and by use of a south-looking radar, chosen to maximize coverage of the Northwest Passage. But, as a consequence, the extreme northern regions are not covered by Radarsat; thus, north of 75° N, ERS-1 has substantial coverage advantage (see figure 6), the Northern Beaufort Sea for example. Data from ERS-1 (out of range of

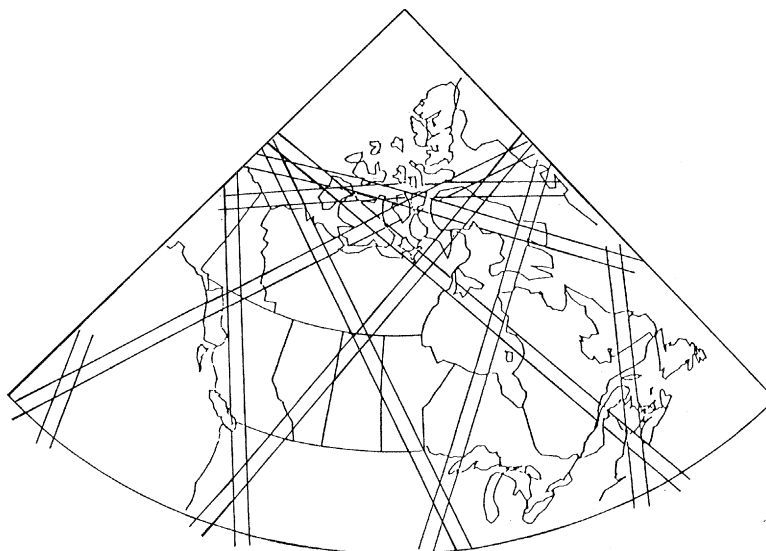


FIGURE 6. Arctic swath coverage for Radarsat SAR. Altitude, 1001.1 km; inclination, 99.48° ; swath, 150 km (l.h.s.). Elevated Sun-synchronous orbit; 1 day of ascending and descending passes in a 3-day subcycle.

Radarsat) will be of importance as input to the ice-generating models being developed for the western Arctic. For this purpose the less frequent coverage of ERS-1 is satisfactory. Therefore, if Radarsat and ERS-1 lifetimes should overlap, these two radar sensors would be complementary.

Radarsat is designed to be more sensitive to weak signal variations than ERS-1. This means that distinction between smooth water and first-year ice will be more reliable from Radarsat. However, for the multiyear ice expected in the far North, ERS-1 performance should be satisfactory. It will be acceptable as a pilot project data source for most mid-Arctic conditions before the availability of Radarsat data. ERS-1 sensitivity should be adequate for most Canadian land applications.

The sensitivity parameter is closely related to the incidence angle parameter. For certain applications, the nominal angle of 22° (ERS-1) is nearly optimal for work such as on soil moisture, yet at just these angles, other applications, such as crop monitoring or iceberg detection, are poorly served. No one incidence angle can satisfy all users.

CONCLUSIONS

Synthetic aperture radar has proved itself to be of value in scientific applications of land and sea observation. Future satellite systems are being planned that would employ SAR systems for experimental and operational Earth remote sensing. Both system technology and application methodology are under active development as we begin this decade.

BIBLIOGRAPHY

- Beal, R. C., DeLeonibus, P. S. & Katz, I. (eds) 1981 *Spaceborne synthetic aperture radar for oceanography*. Johns Hopkins University Press.
- Ford, J. P. *et al.* 1920 *Seasat views North America, the Caribbean, and western Europe with imaging radar (N.A.S.A. Jet Propulsion Laboratory Report no. 80-67)*.
- Fu, L. L. & Holt, B. 1982 *Seasat views oceans and sea ice with synthetic aperture radar (N.A.S.A. Jet Propulsion Laboratory Report no. 81-120)*.
- Long, W. L. 1975 *Radar reflectivity of land and sea*. Lexington Books.
- Raney, R. K. 1982 *Int. J. Remote Sensing* **3**, 243–258.

SEASAT SAR

SCALE 1:500000
FRAME CENTRE 49 6 42 N 123 14 11 W

VANCOUVER, CANADA 100X100 KM
ORBIT 230 13/07/78
25M RESOLUTION 4 LOOKS
SATELLITE HEADING 289.77 DEG
GROUND RANGE

21541
25.063

AZIMUTH



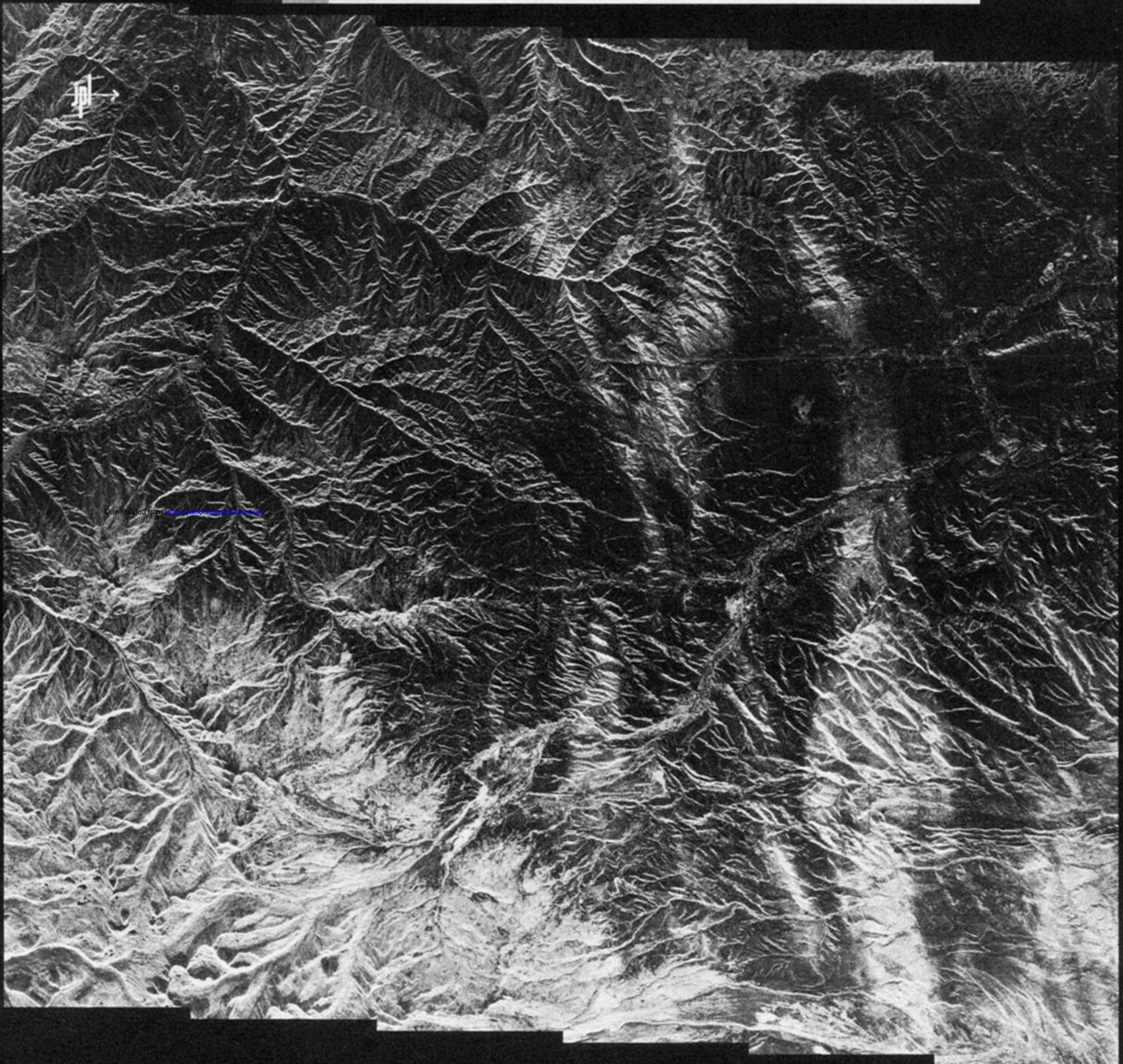
Downloaded from rsta.royalsocietypublishing.org

PHILOSOPHICAL TRANSACTIONS OF THE ROYAL SOCIETY A
MATHEMATICAL PHYSICAL ENGINEERING SCIENCES

CANADA SURSAT PROJECT

DIGITALLY PROCESSED BY 55-3
MERRILL, OPTENTIK & BARR - 176 39.738

FIGURE 2. A Seasat SAR image of Vancouver, B.C.



Downloaded from rsta.royalsocietypublishing.org

NASA JPL SEASAT SAR IMAGE DIGITALLY CORRELATED SPACECRAFT TRACK <---- 204.1 DEGREES DES
NUMBER OF PIXELS 6144 AZIMUTH 5840 RANGE PIXEL SIZE CENTER OF IMAGE 16M AZIMUTH 18M RANGE
REV 0502 GDS SITE EVANSTON, ILL. 1 LAT 41 12'N LON 111 05'W
213 03H07M52S 01 AUG 78 **PROCESSED 07 OCT 80 FILE NO 05020225

FIGURE 3. Effect of recent rain on dry terrain in Wyoming: the streaks are as a result of rain (verified by A. Loomis). Pixel size 16 m × 18 m. (Courtesy of N.A.S.A.)

4

MRL
030681 01

Downloaded from rsta.royalsocietypublishing.org

MATHEMATICAL,
PHYSICAL
& ENGINEERING
SCIENCES

THE ROYAL
SOCIETY

PHILOSOPHICAL
TRANSACTIONS
OF

MATHEMATICAL,
PHYSICAL
& ENGINEERING
SCIENCES

THE ROYAL
SOCIETY

PHILOSOPHICAL
TRANSACTIONS
OF

FIGURE 4. Image displacement of a ship caused by its motion (enlarged image, courtesy of Marconi Ltd).

5

Downloaded from rsta.royalsocietypublishing.org

MATHEMATICAL,
PHYSICAL
& ENGINEERING
SCIENCES

THE ROYAL
SOCIETY

PHILOSOPHICAL
TRANSACTIONS
OF

MATHEMATICAL,
PHYSICAL
& ENGINEERING
SCIENCES

THE ROYAL
SOCIETY

PHILOSOPHICAL
TRANSACTIONS
OF

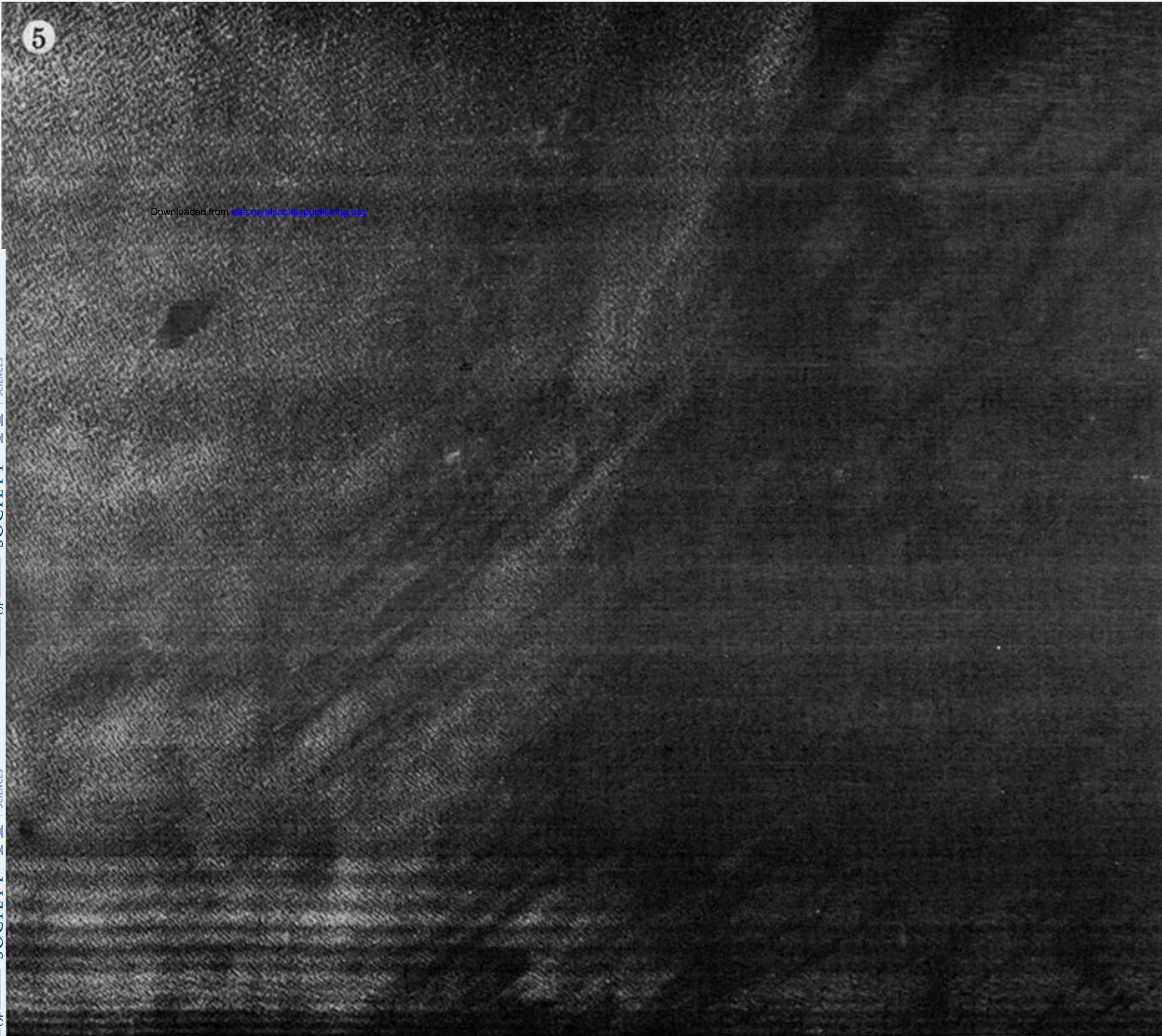


FIGURE 5. Waves in an ice and water environment: waves are visible in the floating ice only (bottom of figure is radar near range).

LARGE MULTI-YEAR
ICE FLOE

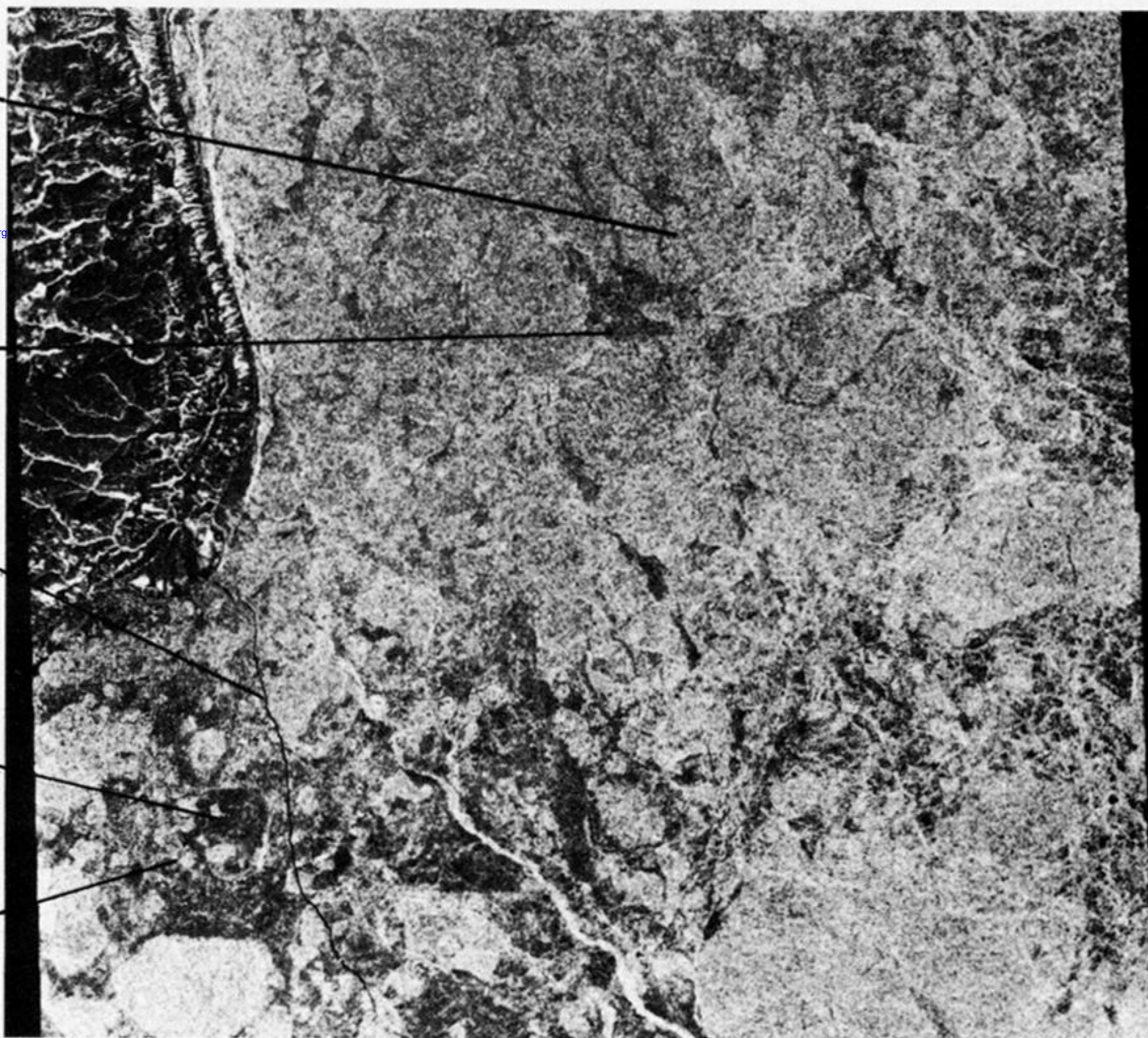
Downloaded from rsta.royalsocietypublishing.org

FIRST-YEAR ICE

NEW LEAD

SMOOTH
FIRST-YEAR ICE

SMALL
MULTI-YEAR FLOES



10 km

RANGE →

AZIMUTH →

CANADA SURSAT PROJECT Digitally processed by
MacDonald, Dettwiler & Assoc., Ltd.

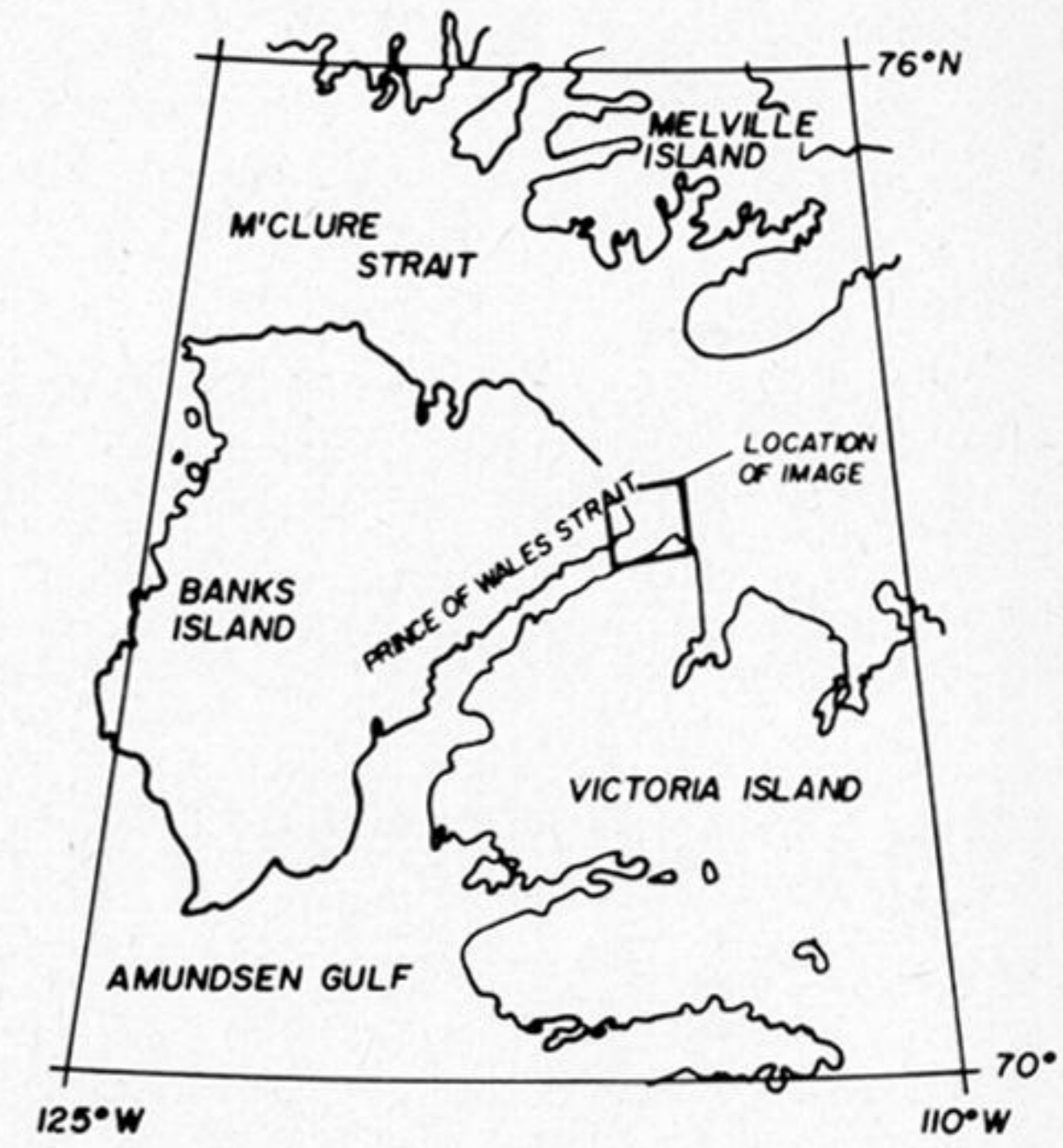


FIGURE 7. Seasat SAR image of Peel Point, N.W.T. (25 m resolution, 4 looks).

PHILOSOPHICAL
TRANSACTIONS
OF
THE ROYAL
SOCIETY
MATHEMATICAL,
PHYSICAL
AND
ENGINEERING
SCIENCES